



Article

Optimizing Precursors and Reagents for the Development of Alkali-Activated Binders in Ambient Curing Conditions

Dhruv Sood and Khandaker M. Anwar Hossain *

Department of Civil Engineering, Ryerson University, Toronto, ON M5B 2K3, Canada; dhruv.sood@ryerson.ca
* Correspondence: ahossain@ryerson.ca

Abstract: Alkali-activated binders (AABs) are developed through the activation of aluminosilicate-rich materials using alkaline reagents. The characteristics of AABs developed using a novel dry-mixing technique incorporating powder-based reagents/activators are extensively explored. A total of forty-four binder mixes are assessed in terms of their fresh and hardened state properties. The influence of mono/binary/ternary combinations of supplementary cementitious materials (SCMs)/precursors and different types/combinations/dosages of powder-based reagents on the strength and workability properties of different binder mixes are assessed to determine the optimum composition of precursors and the reagents. The binary (55% fly ash class C and 45% ground granulated blast furnace slag) and ternary (25% fly ash class C, 35% fly ash class F and 40% ground granulated blast furnace slag) binders with reagent-2 (calcium hydroxide and sodium sulfate = 2.5:1) exhibited desired workability and 28-day compressive strengths of 56 and 52 MPa, respectively. Microstructural analyses (in terms of SEM/EDS and XRD) revealed the formation of additional calcium aluminosilicate hydrate with sodium or mixed Ca/Na compounds in binary and ternary binders incorporating reagent-2, resulting in higher compressive strength. This research confirms the potential of producing powder-based cement-free green AABs incorporating binary/ternary combinations of SCMs having the desired fresh and hardened state properties under ambient curing conditions.

Keywords: alkali-activated binders; supplementary cementitious materials (SCMs); powder-based reagents; geopolymers; ambient curing; strength; microstructure



Citation: Sood, D.; Hossain, K.M.A. Optimizing Precursors and Reagents for the Development of Alkali-Activated Binders in Ambient Curing Conditions. *J. Compos. Sci.* **2021**, *5*, 59. <https://doi.org/10.3390/jcs5020059>

Academic Editor:
Francesco Tornabene

Received: 21 January 2021
Accepted: 13 February 2021
Published: 20 February 2021

Publisher's Note: MDPI stays neutral with regard to jurisdictional claims in published maps and institutional affiliations.



Copyright: © 2021 by the authors. Licensee MDPI, Basel, Switzerland. This article is an open access article distributed under the terms and conditions of the Creative Commons Attribution (CC BY) license (<https://creativecommons.org/licenses/by/4.0/>).

1. Introduction

Ordinary Portland cement (OPC) is the most common cementitious material used in concrete construction industries [1]. The main challenge in fighting climate change comes from the production of cement [2]. As per statistics, one ton of cement is produced per capita each year [3]. The ongoing urbanization, especially in developing countries like China, India, etc., has led to the rapid development of cement concrete industries [4]. The manufacturing process of cement is considered a major source of greenhouse gas emissions [5]. Each ton of cement production releases about 1 kg sulfur dioxide (SO₂), 2 kg nitrogen oxides (NO_x), and 10 kg dust into the atmosphere [3]. There are about 2.8 billion tons of cement products manufactured every year, which in turn are responsible for approximately 5–7% of global carbon dioxide emissions [6,7]. The rapidly growing population and the associated industrialization has created domestic and industrial waste disposal problems. The alarming waste disposal costs and the shortage of landfill sites has led to the illegal disposal of untreated wastes, which is highly detrimental for the environment [8]. The partial substitution of cement with industrial/domestic waste products is already being practiced globally [9,10]. However, the complete replacement of cement with recycled waste and industrial by-products using alkali activation technology/geopolymerization seems to be an optimum solution to reduce global carbon emissions and tackle the waste disposal problems [11].

Alkali-activated materials (AAMs) or geopolymers are cement-free binders made up of aluminosilicate-rich source materials such as fly ash, ground granulated blast furnace slag (GGBFS), metakaolin, and other natural pozzolans incorporating alkaline reagents. In an alkaline medium, the dissolution of Si and Al ions takes place on the surface of source materials [12–14]. Geopolymerization commences when the oxides of silicon and aluminum react with alkaline reagents to form Si-O-Al polymeric chains/bonds [15–17]. The resultant chemical bonding mainly leads to three types of structures/chains: poly(sialate) (-Si-O-Al-O-), poly(sialate-siloxo) (Si-O-Al-O-Si-O), and poly(sialate-disiloxo) (Si-O-Al-O-Si-O-Si-O) [18,19]. The production process of geopolymers requires, comparatively, 60% less energy and releases approximately 80 to 90% less greenhouse gas emissions compared to the production of OPC [15,16,20,21]. Despite the material greenness of geopolymers, their large-scale applications in the construction and infrastructure industries are still scanty [22–24]. This could be associated with the factors involved in the traditional two-part development technique. In this technique, the precursors/source materials and the solution-based reagents are first separately prepared and then mixed to get a wet mix. The first factor is the use of highly alkaline solution-based reagents to enhance the reaction process of the source materials [22]. Handling large quantities of these corrosive solution-based reagents/chemicals for in situ construction applications creates a hostile environment for workers [23,24]. Moreover, low-calcium fly ash-based binders would need heat curing in most cases to enhance the process of geopolymerization to obtain desirable mechanical and microstructural characteristics at required ages [15,16]. The requirement of curing at elevated temperatures not only hinders construction applications but is also energy intensive and thus increases the costs of production, making it less commercially viable [1,25]. In the one-part development technique, the solid/powder form of reagents is utilized to enhance the reaction process of aluminosilicate-rich materials and to achieve a sustainable solution to the abovementioned issues associated with the two-part system. One-part binders are developed without heat curing by adding water to the pre-blended dry mix of precursors and reagents to obtain better mechanical and microstructural characteristics [26]. Moreover, the powder form of reagents is required in significantly smaller quantities than their counterpart alkaline solutions normally used in the two-part system, which would reduce the production costs of the binders, making them commercially viable [27–29].

The production of binders (geopolymers or AAMs) using the one-part development technique or dry-mixing technique is a novel method as evident from the limited existing research studies [27–29]. The fresh and hardened characteristics of any cementitious binder are crucial for its applications in construction industries. These characteristics are significantly influenced by the composition of the source materials/raw materials, reagents/admixtures, water to binder ratio, and curing and placing conditions [30]. The common source materials (fly ash, GGBFS, and metakaolin) usually provide the reactive amorphous silica and alumina but they are frequently facilitated by solid/powder amorphous silica sources [31]. The solid alkali reagent should be capable of raising the pH of the reaction and in turn facilitate the dissolution of ions. These solid-form reagents are generally alkali carbonate, silicate, or hydroxide [32]. As per a recent study, paper sludge after pre-treatment with sodium hydroxide was found to enhance the reactivity of GGBFS and also to act as a filler [33]. Binders consisting of fly ash class F (FA-F), GGBFS, and hydrated lime incorporating anhydrous sodium silicate and sodium hydroxide as solid-form reagents were developed [34–36]. The compressive strength and workability of one-part binders was found to be about 5 MPa and 35% lower, respectively, than their two-part counterparts of a similar composition. Binders developed with FA-F only exhibited the formation of sodium-alumino-silicate-hydrate (N-A-S-H)-binding phases/gels and/or a low-calcium N(C)-A-S-H gel [34–37]. The setting times of the binders increased when GGBFS was incorporated in the mixes [21]. GGBFS-based binders using a solution-based reagent exhibited faster setting than those using powder-form reagents [38]. This incorporation of slag as/in a source material resulted in the formation of cement hydration-like binding phases such

as calcium-silicate-hydrate (C-S-H) or calcium-alumino-silicate-hydrate (C-A-S-H) [39–42]. These gels/binding phases are denser than conventional sodium-alumino-silicate-hydrate gels and hence improve the microstructure of the binders, resulting in enhanced compressive strengths [43]. The influence of composite reagents on the fresh state and hardened characteristics of one-part binders was investigated in a research study [44]. The partial replacement of sodium silicate anhydrous with sodium carbonate slightly decreased the short-term strength of binders. The reason for the strength reduction was attributed to the introduction of unfavorable porosity by the incorporation of sodium carbonate. Additionally, this resulted in the reduced environmental impact of sodium silicate. The environmental impact of one-part binders was found to be lower than their traditional two-part counterparts. The main difference between the one-part and two-part techniques was inferred to be the difference in the dissolution rate of Si and Al in the system [31].

This article further contributes to the existing research studies on the development one-part AAMs highlighting the hindrance observed in the conventional two-part system. A comprehensive study to develop alkali-activated binders (AABs) based on a dry mixing technique is planned and conducted to optimize mix compositions to produce cement-free composites [11]. The research is focused on the synthesis of sustainable AABs with improved fresh and hardened state characteristics under ambient curing conditions. The influences of mono/binary/ternary combinations/proportions of SCMs, types/dosages of reagents (powder/solution), reagent component ratio, and the fundamental chemical ratios ($\text{SiO}_2/\text{Al}_2\text{O}_3$, $\text{Na}_2\text{O}/\text{SiO}_2$, CaO/SiO_2 , and $\text{Na}_2\text{O}/\text{Al}_2\text{O}_3$) present in the precursor and reagents on workability (slump flow spread) and compressive strength have been investigated to suggest suitable AAB mix compositions for practical use. The suitable mix compositions are determined in terms of optimum proportion/combinations of precursors and the optimum dosage/reagent component ratio of the reagents to achieve the desired flow and strength characteristics. The novelties of this research include the development of one-part binders using a dry mixing technique under ambient curing and finding the optimal reagent component ratios/chemical ratios in combination with precursor combinations to achieve satisfactory fresh and hardened state properties. In addition, the suggested binder mixes will ensure a reduced environmental impact compared to their conventional two-part counterparts by eliminating the need for heat curing and using powder-form reagents in lesser quantities. The recommendations of this paper will surely benefit engineers and designers to further develop the technology and produce AABs for practical applications.

2. Experimental Program, Methods, and Materials

This research was initiated with the development of AABs using the conventional technique of two-part production. The need for heat curing to achieve the desired strength of 40 MPa to 50 MPa at the required 28/56 days and the corrosive nature of the highly alkaline reagents (used in two-part production) encouraged the incorporation of powder-based reagents in the development of one-part binders. Additionally, these solid/powder forms of reagents were required in significantly lesser quantities than their solution-based reagent counterparts, which reduced the cost of production and bolstered the commercialization of such binders. A total of 44 AAB mixes were produced in an extensive investigation to determine the optimal mono/binary/ternary combination/proportion of SCMs, superior performing reagents, types/dosages of reagents (powder/solution based), and the optimal reagent component ratio based on compressive strength and workability properties.

2.1. Aluminosilicate-Rich Materials

Aluminosilicate-rich materials, such as high-calcium fly ash class C (FA-C), low-calcium fly ash class F (FA-F), and GGBFS, were used as source materials/precursors for the development of AABs. Additionally, general use (type GU) cement was used for producing control binder mixes. The chemical compositions obtained through X-ray fluorescence spectrometer

analysis and the physical properties of these materials are presented in Table 1. The grain size distribution of SCMs and cement is presented in Figure 1.

Table 1. Chemical and physical properties of precursors and cement.

Chemical Composition (%)	Fly Ash Class C (FA-C)	Fly Ash Class F (FA-F)	Ground Granulated Blast Furnace Slag (GGBFS)	Cement
SiO ₂	36.53	55.66	35.97	19.35
Al ₂ O ₃	18.26	22.09	9.18	5.31
Fe ₂ O ₃	5.66	4.26	0.50	3.10
CaO	20.97	7.97	38.61	62
MgO	5.08	1.16	10.99	3
K ₂ O	0.68	1.49	0.36	-
Na ₂ O	4.04	4.10	0.28	0.23
MnO	0.03	0.03	0.25	-
TiO ₂	1.26	0.61	0.39	-
P ₂ O ₅	0.96	0.43	0.01	-
L.O.I.	2.18	1.05	0.74	2.40
Physical properties	FA-C	FA-F	GGBFS	Cement
Density (g/cm ³)	2.61	2.02	2.87	3.15
Retained on 45 μ, %	-	18	-	3
Blaine fineness (m ² /kg)	315	306	489.30	410

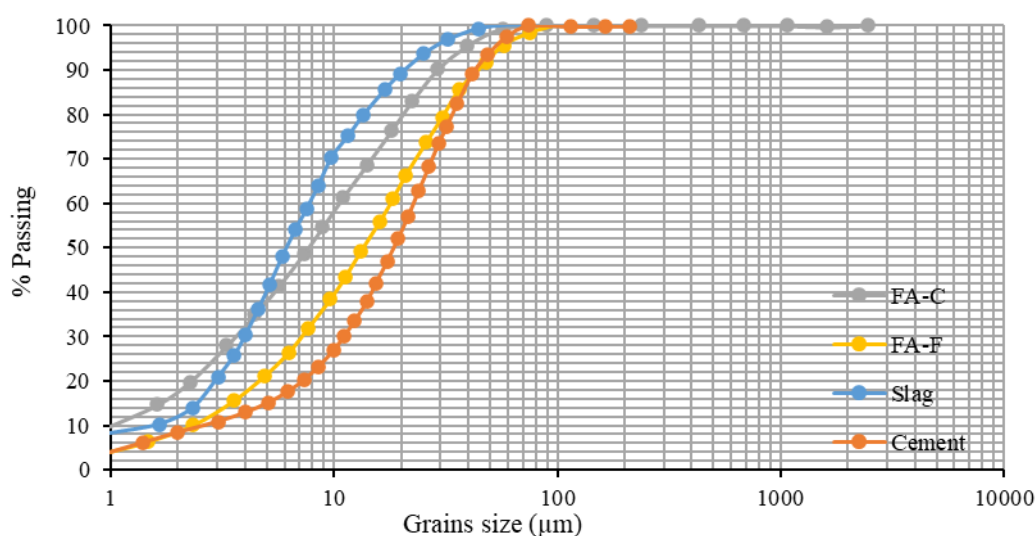


Figure 1. Grain size gradation of supplementary cementitious materials (SCMs) and cement.

2.2. Reagents

In total, six different types/combinations of reagents were used in this research. Four solid/powder and two solution-based reagents were used to initiate/enhance the reaction process of the aluminosilicate-rich materials. The physical and chemical properties of the reagents are listed in Table 2. Reagent-p (solution form) was composed of 8.0 M sodium hydroxide (NaOH) and grade D sodium silicate solutions. Reagent-q (solution form) consisted of 8 M NaOH solution. The most common molarity and dosage of the solution-based reagents (NaOH and grade D sodium silicate) used in the existing literature were selected to see their effect and feasibility for different combinations/proportions of precursors (FA-C, FA-F, and slag) [2]. Reagent-1a (powder form) was prepared by mixing calcium hydroxide and sodium silicate (sodium silicate grade G) in powder/solid form. The components of reagent-1b (powder form) were calcium hydroxide and sodium silicate (sodium silicate grade GD). Reagent-1 was composed of a combination of calcium hydroxide (Ca(OH)₂) and sodium meta-silicate (Na₂SiO₃·5H₂O). The constituents of reagent-2 were calcium

hydroxide and sodium sulfate (Na_2SO_4). The components of the reagents were mixed as per the mix proportions. The incorporation of a multi-component reagent was considered in this study because the utilization of single component sodium metasilicate alone causes expansion cracks in the specimens, as observed in this investigation. The occurrence of expansion cracks can be attributed to the presence of excess volatile sodium in the system, resulting in reduced compressive strengths and even splitting of cubic specimens before testing. The addition of calcium hydroxide to sodium metasilicate not only added to the stability of the mixes but also resulted in the formation of sodium hydroxide which further enhanced the reaction process. These reagents, of lab grade standard, were procured from National Silicates and Westlab, Canada.

Table 2. Physical and chemical properties of reagents.

Reagent Type (R. Type)	Reagent Components (R. Components)		Modulus Ratio (MR = $\text{SiO}_2/\text{Na}_2\text{O}$)	Specific Gravity (g/cm^3)		pH		Purity (%)
P (solution)	Na_2SiO_3	NaOH	2	1.53	2.13	12.9	14	95–100
q (solution)	NaOH		-	2.13		14		95–100
1a (powder)	$\text{Ca}(\text{OH})_2$	Na_2SiO_3 (Grade G)	3.22	2.24	0.70	12.4–12.6	11.3	95–100
1b (powder)	$\text{Ca}(\text{OH})_2$	Na_2SiO_3 (Grade GD)	2	2.24	0.73	12.4–12.6	12.3	95–100
1 (powder)	$\text{Ca}(\text{OH})_2$	$\text{Na}_2\text{SiO}_3 \cdot 5\text{H}_2\text{O}$	1	2.24	1.81	12.4–12.6	14	95–100
2 (powder)	$\text{Ca}(\text{OH})_2$	Na_2SO_4	-	2.24	2.70	12.4–12.6	7	95–100

2.3. Superplasticizers

A polycarboxylate ether-based superplasticizer (SP) was used with a multi-component reagent/activator to enhance/initiate the reaction process of the source materials, whereas a naphthalene-based superplasticizer was incorporated in the case of a single component reagent/activator. The physical and chemical characteristics of the superplasticizers are listed in Table 3.

Table 3. Physical and chemical characteristics of superplasticizers.

ID	Industrial Name	Chemical Base	Color	pH	Specific Gravity (g/cm^3)	Approx. Solids (%)
1	Master Rheobuild 1000 NT	Naphthalene	Dark brown	6–10	1.17–1.22	41
2	Adva Cast 575	Polycarboxylate	Blue	6	1.06	40

2.4. Mix Proportions

The mix proportions of two-part (2 mixes) and one-part (42 mixes consisting of 25 mono and 17 binary/ternary) AABs and a control mix (FP_C) are presented in Table 4, Table 5a,b with their mix designations and the fundamental chemical ratios ($\text{SiO}_2/\text{Al}_2\text{O}_3$, $\text{Na}_2\text{O}/\text{SiO}_2$, CaO/SiO_2 , and $\text{Na}_2\text{O}/\text{Al}_2\text{O}_3$) present in the precursors and the reagents.

The binder mix compositions were developed based on the fundamental concepts of water/binder ratio, reagent/binder ratio, and reagent component ratio used in the conventional two-part development technology, as presented in Table 4. The paste component of a standard engineered cementitious composite (ECC) mix developed at Ryerson University was chosen as the control mix for this study [45,46], as one of the goals of this research is to

develop an alkali-activated zero cement-based ECC. The total fly ash content varied from 50 to 60% and the amount of GGBFS varied from 40 to 50% by mass of the total binder content in the binary/ternary AAB pastes, similar to the fly ash and cement content in the control binder (ECC paste mix (FP_C)), as indicated in Table 5b. The water to binder ratio for 42 one-part AABs varied from 0.35 to 0.375 to obtain a minimum slump flow (mini-slump) spread of 155 mm and was kept constant at 0.27 for the control paste, as previously established. The dosage of SP was kept constant at 0.01 and 0.006 of total binder content for the AAB paste and control paste, respectively, as it is acidic in nature and, thus, should not act differently in varying mix compositions with alkaline reagents.

Table 4. Mix proportions of two-part binders (two mixes with FA-C).

Mix Designation	FA-C (Binder *)	R. Type	R. Component Ratio	Reagent/Binder	Extra Water	Water/Total Solids	28-Day Compressive Strength (MPa)
CS _B -1	1	p	2.5:1	0.35	0.014	0.20	56.3
CS _B -2	1	q	1	0.29	0	0.20	26.3

* All numbers are mass ratios of binder except water/total solids; C: FA-C, S_B: solution-based reagent.

Table 5. (a) Mix proportions for one-part mono binders (25 mixes). (b). Mix proportions for one-part binary and ternary binders (18 mixes).

Table 5a												
Mix des.	Total SCMs (Binder)	SCMs				R. Component Ratio	R./B	Chemical Ratios (SCMs + Reagent)				Compressive Strength (MPa) 28 Days
		P _C	FA-C	FA-F	GGBFS			SiO ₂ /Al ₂ O ₃	Na ₂ O /SiO ₂	CaO /SiO ₂	Na ₂ O /Al ₂ O ₃	
C-1-1a	1	0	1	0	0	7.5:1	0.09	2.02	0.11	0.77	0.23	13.3
C-2-1a	1	0	1	0	0	5:1	0.09	2.03	0.11	0.76	0.23	16.7
C-3-1a	1	0	1	0	0	2.5:1	0.09	2.05	0.11	0.72	0.24	18.0
C-4-1a	1	0	1	0	0	1:1	0.09	2.08	0.12	0.66	0.25	17.5
C-5-1a	1	0	1	0	0	0:1	0.09	2.16	0.12	0.53	0.27	13.5
C-6-1a	1	0	1	0	0	1:2.5	0.09	2.11	0.12	0.61	0.26	17.3
C-7-1b	1	0	1	0	0	1:2.5	0.09	2.10	0.13	0.61	0.27	13.3
C-8-1b	1	0	1	0	0	0:1	0.09	2.13	0.13	0.54	0.29	5.0
C-8 ⁿ -1b	1	0	1	0	0	0:1	0.09	2.13	0.13	0.54	0.29	5.4
C-9-1b	1	0	1	0	0	1:1	0.09	2.07	0.12	0.67	0.25	11.5
C-10-1	1	0	1	0	0	2.5:1	0.09	2.02	0.12	0.73	0.24	21.0
C-11-1	1	0	1	0	0	1:1	0.09	2.04	0.13	0.68	0.26	9.5
C-12-1	1	0	1	0	0	1:2.5	0.09	2.05	0.13	0.63	0.27	3.6
F-1-1	1	0	0	1	0	1:2.5	0.09	2.56	0.09	0.18	0.23	4.3
F-2-1	1	0	0	1	0	1:1	0.09	2.55	0.08	0.22	0.22	4.8
F-3-1	1	0	0	1	0	2.5:1	0.09	2.54	0.08	0.25	0.20	5.5
S-1-1	1	0	0	0	1	0:1	0.09	4.06	0.04	1.04	0.17	52.5
S-1 ⁿ -1	1	0	0	0	1	0:1	0.09	4.06	0.04	1.04	0.17	32.9
S-2-1	1	0	0	0	1	1:2.5	0.09	4.02	0.03	1.11	0.13	29.3
S-3-2	1	0	0	0	1	2.5:1	0.12	3.92	0.08	1.30	0.32	34.1
S-4-2	1	0	0	0	1	1:1	0.12	3.92	0.14	1.23	0.54	23.5
S-5-2	1	0	0	0	1	1:2.5	0.12	3.92	0.19	1.16	0.76	17.5
C-13-2	1	0	1	0	0	2.5:1	0.12	2.00	0.18	0.80	0.37	15.2
C-14-2	1	0	1	0	0	1:1	0.12	2.00	0.24	0.73	0.48	13.3
C-15-2	1	0	1	0	0	1:2.5	0.12	2.00	0.29	0.66	0.59	13.0

Table 5. Cont.

Table 5b												
Mix des.	Total SCMs + P _C (Binder*)	P _C	SCMs			R. Component Ratio	R/B	Chemical Ratios (SCMs + Reagent)				Compressive Strength (MPa) 28 Days
			FA-C	FA-F	GGBFS			SiO ₂ /Al ₂ O ₃	Na ₂ O/SiO ₂	CaO/SiO ₂	Na ₂ O/Al ₂ O ₃	
CS-1-1	1	0	0.55	0	0.45	0:1	0.09	2.65	0.10	0.77	0.26	5.5
CS-2-1	1	0	0.55	0	0.45	1:2.5	0.09	2.62	0.09	0.84	0.23	47.8
CS-3-2	1	0	0.55	0	0.45	2.5:1	0.12	2.56	0.14	1.02	0.35	56.3
CS-4-2	1	0	0.55	0	0.45	1:1	0.12	2.56	0.19	0.95	0.49	6.5
FS-1-1a	1	0	0	0.55	0.45	2.5:1	0.09	2.92	0.06	0.58	0.16	20.3
FS-2-1	1	0	0	0.55	0.45	2.5:1	0.09	2.90	0.06	0.59	0.17	25.3
FS-3-1	1	0	0	0.55	0.45	1:2.5	0.09	2.93	0.07	0.51	0.20	23.8
FS-4-2	1	0	0	0.55	0.45	2.5:1	0.12	2.87	0.11	0.64	0.31	4.3
CFS-1-1	1	0	0.25	0.35	0.40	0:1	0.09	2.77	0.09	0.53	0.24	3.5
CFS-2-1	1	0	0.25	0.35	0.40	2.5:1	0.09	2.72	0.07	0.68	0.18	35.0
CFS-3-1	1	0	0.25	0.35	0.40	1:1	0.09	2.73	0.07	0.63	0.20	4.2
CFS-4-1	1	0	0.25	0.35	0.40	1:2.5	0.09	2.75	0.08	0.59	0.22	41.3
CFS-5-2	1	0	0.25	0.35	0.40	2.5:1	0.12	2.69	0.12	0.73	0.32	52.2
CS-2N-1	1	0	0.5	0	0.5	1:2.5	0.09	2.71	0.08	0.87	0.23	41.5
CFS-4N-1	1	0	0.25	0.25	0.5	1:2.5	0.09	2.86	0.07	0.69	0.21	38
CS-3N-2	1	0	0.5	0	0.5	2.5:1	0.12	2.64	0.13	1.02	0.35	43.5
CFS-5N-2	1	0	0.25	0.25	0.5	2.5:1	0.12	2.80	0.12	0.84	0.33	39.1
FP _C	1	0.45	0	0.55	0	-	-	2.70	0.06	0.82	0.16	40.3

* All numbers are mass ratios of binder; binder denotes supplementary cementitious materials (SCMs); P_C: Portland cement; C: FA-C; F: FA-F; S: GGBFS; N denotes mixes with equal mass proportion of total fly ash and GGBFS; last alphanumeric character after hyphen denotes reagent type. ^a Mixes with naphthalene-based SP, all others had carboxylate-based SP.

2.5. Preparation of Geopolymer Binders with Casting and Curing of Specimens

The aluminosilicate-rich materials (binder constituents) and the reagents required for each mix composition were weighed as per the proportions given in the Table 4, Table 5a,b. The reagent components were first mixed thoroughly to form a multi-component reagent/activator which was then added to the rigorously blended binder constituents. The complete binder system was then dry mixed (in the case of solid/powder form of reagents) for about 3 min in a shear mixer. After 3 min of dry mixing, two-thirds of the required water were gradually added to the mix. Then a superplasticizer mixed with the remaining amount of water was gradually added for a period of 2–3 min. The total mixing procedure lasted about 10–12 min. In the case of two-part AAB development (conventional technique), thoroughly mixed alkaline solution components of the reagent were added to the blended binder constituents for about 3–4 min in a shear mixer. Extra water was then gradually added for about 1–2 min if required as per the mix design. The entire mixing operation lasted about 8–10 min.

At least 12 cube specimens with dimensions of 50 mm × 50 mm × 50 mm were prepared for each binder composition. The cube molds were kept in the curing room maintained at a temperature of 23 ± 3 °C and 95 ± 5% relative humidity (RH). The cubes were demolded after 24 h of casting and were kept in the curing chamber until the day of testing. For the conventional technique, the molds were sealed and kept in the oven maintained at 60 °C for 24 h. After 24 h of heat curing, molds were carefully taken out from the oven and left undisturbed until cooled. The cubes were then de-molded after the cooling period and left in ambient laboratory conditions until the day of testing.

2.6. Test Methods

The compressive strength test using cube specimens (Figure 2a) at 7, 14, 28, and 56 days was conducted according to ASTM C109/C109M [47]. The slump flow spread characteristics of the mixes, as presented in Figure 2b, were assessed through a mini-slump cone test in compliance with ASTM C1437 [48]. The morphology and microstructural characteristics of the binders were studied using scanning electron microscope (SEM) and energy dispersive spectroscopy (EDS) analysis. The specimens were taken from the core of the failed compression test cubes at 28 days. The specimens were ground and softly polished with sandpaper down to 30 μm . A gold coating was applied on the specimens to make the surface conductive. The fracture surface was studied using both secondary electrons (SEs) and back-scattered electrons (BSEs) at 20 kV. The morphology of the specimens was studied at 100X (100 μm) and the reaction product assessment was done at 2000X (10 μm). The specimen preparation XRD consisted of grinding the specimen taken from the core of the failed compression cubes. The ground specimen was passed through a 200-mesh sieve. A Bruker D8 Endeavor diffractometer equipped with a Cu X-ray source and operating at 40 kV and 40 mA; range 10–70 deg θ ; step size 0.02 deg 2° ; time per step 0.5 sec; fixed divergence slit, angle 0.30; sample rotation 1 rev/sec was used to identify the mineral phases using the PDF4/Minerals ICDD database.



Figure 2. Test set-up for (a) compressive strength, (b) mini-slump flow.

3. Results and Discussion

3.1. Analysis of Compressive Strength

The compressive strength development of 44 different binders with ages of 7, 14, 28, and 56 days is described to illustrate the influence of various mix design parameters reflecting mono, binary, and ternary combinations of SCMs as well as types, proportions, and dosages of powder/solution-form reagents and chemical ratios. All the binder mixes exhibited a ratio of $\text{Na}_2\text{O}/\text{Al}_2\text{O}_3$ of less than one (Table 5a,b), however, the investigation for efflorescence was not part of this study. It has been observed in previous studies that a ratio of $\text{Na}_2\text{O}/\text{Al}_2\text{O}_3 < 1$ resulted in the consumption of sodium in the reaction process and in turn prevented efflorescence [49]. The 28-day compressive strengths of all the binders are presented in Tables 4 and 5a,b.

3.1.1. Influence of Solution-Based Reagent Types on Fly Ash Class C-Based Mono Binders

The mix composition $\text{CS}_B\text{-1}$ (Table 4) incorporating reagent-p (solution form) obtained compressive strengths of 50.0 MPa and 56.3 MPa at 7 and 28 days, respectively. The inclusion of reagent-q (solution form) in fly ash class C (mix $\text{CS}_B\text{-2}$) lead to lower strengths 20.8 and 26.3 MPa at both 7 and 28 days. The substantially higher (114 to 140%) strength in the case of reagent-p can be attributed to its silicate component (Modulus ratio (MR): $\text{SiO}_2/\text{Na}_2\text{O} = 2$). This facilitated the dissolution process of Si and Al in the system by

providing comparatively more of these ions and alkalinity for geopolymerization. Both the binder systems (CS_B-1 and CS_B-2), however, required heat curing conditions to achieve those strengths at the respective ages. Therefore, the use of powder-based reagents was incorporated to enhance the reaction process of the precursors/source materials.

3.1.2. Influence of Powder-Based Reagents on Fly Ash Class F and C Mono Binders

The incorporation of powder-based reagents to develop binders was initiated based on previous research works indicating low compressive strengths of one-part binders at 28 days [49]. In this study, to improve the compressive strength, the production of binders using powder-based reagents commenced with the use of a precursor high in calcium content (FA-C) and reagent-1a, incorporating the same component ratio of $\text{Ca}(\text{OH})_2:\text{Na}_2\text{SiO}_3 = 7.5:1$ as used in a previous study [50]. The silicate component was gradually increased to see its effect on the compressive strength of FA-C binders. Additionally, the use of solution-based reagents having a high silicate content ($\text{NaOH}:\text{Na}_2\text{SiO}_3 = 1:2.5$) resulted in high compressive strength.

The influences of reagents (1a and 1b) on the compressive strengths of FA-C-based mono binders are presented in Figure 3. For mono mixes with fly ash class C with reagent-1a (Table 5a), considerable improvements in 28-day compressive strengths from 13.25 MPa to 17.5 MPa were observed when the silicate ratio ($\text{SiO}_2/\text{Al}_2\text{O}_3$) increased from 1:7.5 to 1:1 (mixes C-1-1a, C-2-1a, C-3-1a, and C-4-1a), as shown in Figure 3. A high silica content in the system facilitates the process of geopolymerization by supplying the required silicate ions. However, when using sodium silicate (Grade G) as a single component reagent for mix composition C-5-1a, the compressive strength dropped by 22% (from 18 MPa to 13.5 MPa) at 28 and 56 days. This could be due to the possible leaching of Si ions from the system because of a high degree of polymerization as a consequence of a high $\text{SiO}_2/\text{Al}_2\text{O}_3$ ratio of 2.16 and low CaO/SiO_2 ratio of 0.53. Another reason could be the presence of high/excessive sodium (Na) in the system which resulted in the formation of expansive product and hence a reduction in compressive strength.

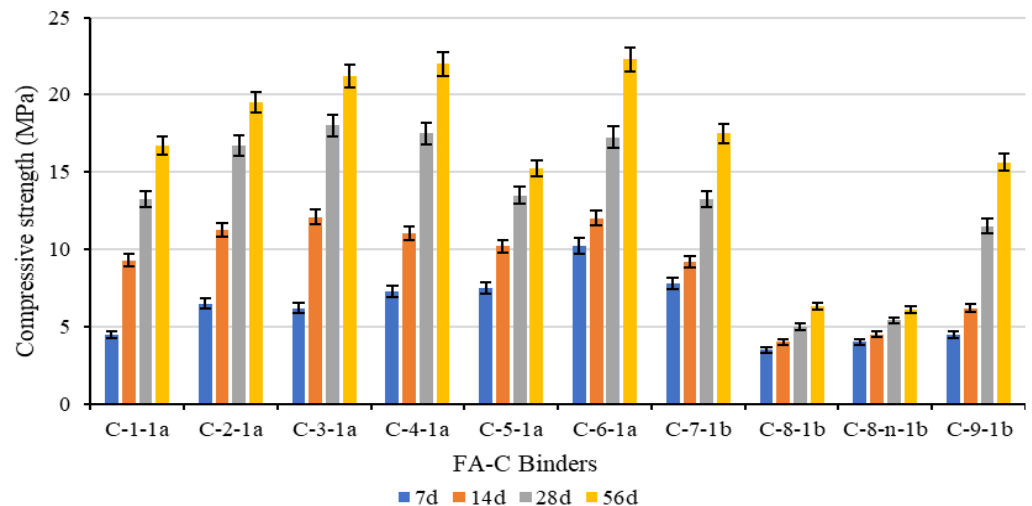


Figure 3. Influence of reagents (1a and 1b) on FA-C binders.

The compressive strengths for FA-C-based binders with reagent-1a and 1b ranged from 5 MPa to 18 MPa at 28 days (Figure 3). The reagent component ratio ($\text{Ca}(\text{OH})_2:\text{Na}_2\text{SiO}_3 = 1:2.5$) was determined to be the superior composition for reagent-1a as it resulted in a maximum compressive strength of 22.3 MPa at 56 days among the mixes with reagent-1a. A similar trend was observed for reagent-1b, with the same component ratio ($\text{Ca}(\text{OH})_2:\text{Na}_2\text{SiO}_3 = 1:2.5$) being superior, as apparent from Figure 3. However, reagent-1b resulted in slightly lower compressive strengths due to its lower silica modulus, as indicated in Table 2.

A gradual gain in compressive strength with age (from 7 days to 56 days) can be seen for all the binders incorporating reagent-1a and 1b (Figure 3). However, the mix compositions C-8-1b and C-8-n-1b exhibited a low compressive strength at all ages with maximum strengths of 6.3 MPa and 6.1 MPa at 56 days. These low strengths could be due to their low CaO/SiO₂ ratio of 0.54 and high SiO₂/Al₂O₃ ratio of 2.13, resulting in the possible leaching of Si and Al ions from the system.

The influence of reagent-1 and reagent-2 with varying reagent component ratios depicted in Table 5a on FA-C-based binders can be seen from Figure 4. A gradual gain in compressive strength with age (from 7 days to 56 days) was observed for all the binders incorporating reagents 1 and 2. The component ratio (Ca(OH)₂/Na₂SiO₃·5H₂O = 2.5:1) for reagent-1 performed the best in terms of compressive strength among all the FA-C binders. This can be attributed to the high alkalinity of sodium metasilicate (pH = 14) incorporated in this multi-component reagent. However, a further increase in alkalinity in mixes C-11-1 and C-12-1 as compared to the mix C-10-1, and a decrease in the CaO/SiO₂ ratio from 0.73 to 0.63 for the same mixes, resulted in compressive strength reductions by 53 to 83% at 28/56 days, respectively, with possible leaching of Si and Al ions. A lower increase in compressive strength from 7 to 56 days was observed for C-12-1 compared to the others (Figure 4). In the case of reagent-2, the compressive strengths of binders C-13-2 to C-15-2 decreased by 10 to 15% with the reduction of calcium content (Ca(OH)₂/Na₂SO₄ from 2.5:1 to 1:2.5) and the corresponding decrement in alkalinity associated with calcium hydroxide. Reagent-1 with component ratios of Ca(OH)₂/Na₂SiO₃·5H₂O of 2.5:1 and 1:2.5 and reagent-2 with a component ratio of Ca(OH)₂/Na₂SO₄ of 2.5:1 were found to be the most suitable for different precursors and their combinations/proportions in terms of better compressive strength development.

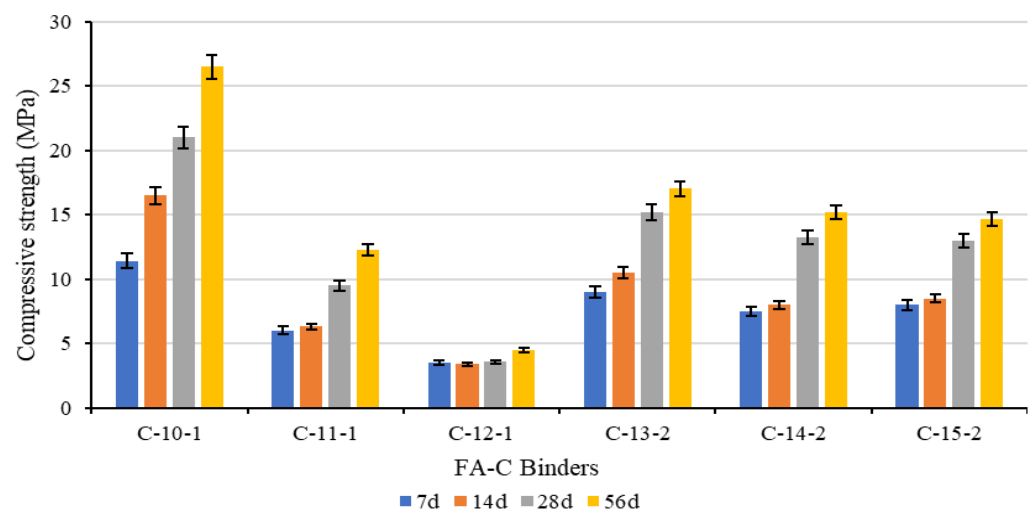


Figure 4. Influence of reagents (1 and 2) on fly ash class C (FA-C).

Overall, the 28-day compressive strength of FA-C-based mono binders (presented in Table 5a) with all powder-based reagents (type 1a, 1b, 1, and 2) varied from 3.56 MPa to 21 MPa (Figures 3 and 4). The mono binders incorporating fly ash class F (FA-F) and different combinations/dosages of reagents (mixes F-1-1, F-2-1, and F-3-1, presented in Table 5a) resulted in low 28-day compressive strength ranging from 4.0 to 5.5 MPa and showed long setting times (>24 h). This can be attributed to possible leaching of Si and Al ions from the system and due to their low CaO/SiO₂ ratio ranging from 0.18 to 0.25. It could also be due to the low reactivity potential of FA-F as the strong glassy chain of Si-Al consisting of high Si and Al and low Ca needs to be disintegrated first to initiate the reaction process [51].

3.1.3. Influence of Powder-Based Reagents on GGBFS-Based Mono Binders

Figure 5 shows the compressive strength development of GGBFS-based binders incorporating reagents (1 and 2) from 7 to 56 days. A gradual gain in compressive strength with age (from 7 days to 56 days) was observed for all the binders incorporating reagent-1 and 2. The GGBFS-based mono binders incorporating reagent-1 and 2 obtained compressive strengths varying from 17.5 MPa to 52.5 MPa at 28 days. The characteristic high alkalinity of sodium metasilicate (pH: 14) led to the enhanced dissolution of Si and Al ions and the high calcium content (38.61%) in GGBFS facilitated providing Ca^{2+} ions, resulting in the formation of both C-S-H and C-A-S-H products responsible for high strengths at early ages. The mix S-1-1 obtained a high strength of 55 MPa at 56 days, as indicated in Figure 5. The incorporation of a naphthalene-based superplasticizer in the mix S-1ⁿ-1 led to 36 to 38% lower compressive strength than S-1-1 (made with polycarboxylate-based SP) at early ages of 7, 14, and 28 days but resulted in similar strength at 56 days, as can be observed in Figure 5. This might be attributed to the retarding effect of naphthalene-based SP. The binder S-2-1 obtained 38 to 54% lower compressive strength than S-1-1 (reagent ratio of $\text{Ca}(\text{OH})_2:\text{Na}_2\text{SiO}_3\cdot 5\text{H}_2\text{O} = 0:1$) due to its lower silicate component ratio ($\text{Ca}(\text{OH})_2:\text{Na}_2\text{SiO}_3\cdot 5\text{H}_2\text{O} = 1:2.5$) and reduced associated alkalinity. Though higher compressive strengths were observed for S-1-1 mixes, some specimens exhibited expansion cracks and even splitting of cube specimens in some cases, as indicated in Figure 6. Therefore, a reagent component ratio of $\text{Ca}(\text{OH})_2:\text{Na}_2\text{SiO}_3\cdot 5\text{H}_2\text{O} = 1:2.5$ was judged to be superior among the two reagent-1 compositions. For reagent-2, the component ratio ($\text{Ca}(\text{OH})_2/\text{Na}_2\text{SO}_4 = 2.5:1$) was determined to be the best performing based on compressive strengths. As the calcium content and the associated alkalinity with calcium hydroxide decreased in mixes S-4-2 and S-5-2, 20 to 50% lower compressive strengths were obtained at 28 and 56 days, respectively, as indicated in Figure 5.

3.1.4. Influence of Powder-Based Reagents on Binary Combinations of FA-C and GGBFS Binders

Figure 7 shows the compressive strength development of binders incorporating FA-C and GGBFS and reagent-1 and 2 from 7 to 56 days compared to control cement (FPC) paste. In general, compressive strength increased with the increase in age and 28-day compressive strengths were higher for binary binders compared to the control mix, except for CS-1-1 and CS-4-2. CS-4-2 shows the lowest compressive strength at all ages due to the low Ca content of the reagent ($\text{CH}/\text{Na}_2\text{SO}_4 = 1:1$). Reagent-2 ($\text{Ca}(\text{OH})_2:\text{Na}_2\text{SO}_4 = 2.5:1$) performed better than reagent-1 ($\text{Ca}(\text{OH})_2:\text{Na}_2\text{SiO}_3\cdot 5\text{H}_2\text{O} = 1:2.5$) in terms of compressive strengths. The binder CS-3-2 obtained the highest compressive strength of 64.2 MPa at 56 days among all the binary binders, as indicated in Figure 7. The compressive strength of binary binders (FA-C + GGBFS) with reagent-1 and 2 ranged between 6.5 MPa and 56.3 MPa at 28 days. The rate of strength gain was faster in the case of reagent-2 because of the higher calcium content in the system and the corresponding predominant formation of C-A-S-H gels, along with additional C-S-H binding phases. However, a 5% higher GGBFS content in the compositions CS-2N-1 and CS-3N-2 resulted in 13 to 23% lower strengths than their CS-2-1 and CS-3-2 counterparts with the same reagent component ratios at 28 days. There seems to be a threshold for the GGBFS content in the system. The possible incompatibility between the predominant C-A-S-H/C-S-H gel and the N-A-S-H gel formed (as observed in SEM and EDS analyses explained later), along with the probable development of internal cracks owing to expansion/instability, because of a high calcium content (higher GGBFS content) in the system, which resulted in reduced compressive strength.

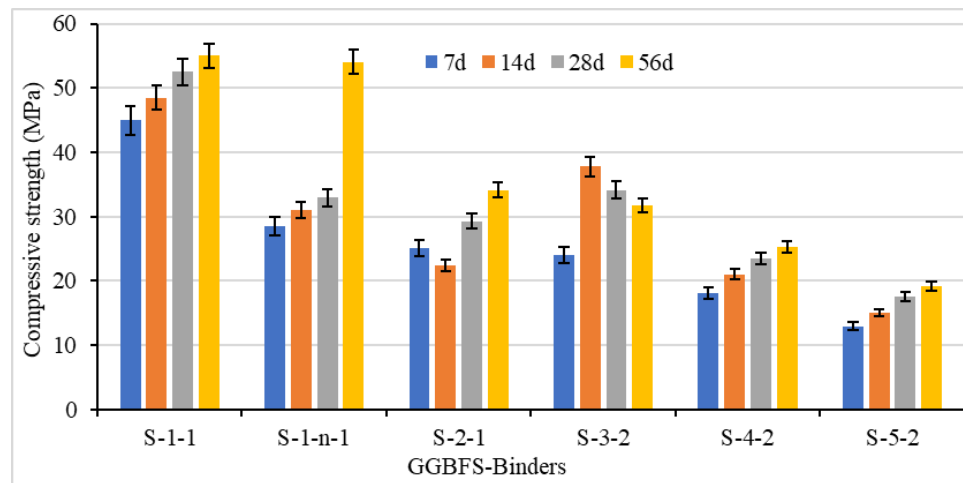


Figure 5. Influence of reagents (1 and 2) on GGBFS binders.

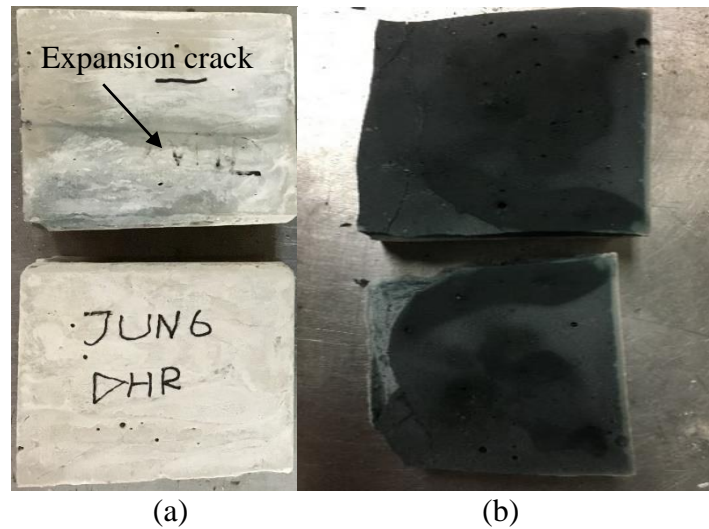


Figure 6. (a) Expansion crack in cube; (b) cracked cube pieces along the crack for mono ground granulated blast furnace slag (GGBFS) binders with reagent $\text{Na}_2\text{SiO}_3 \cdot 5\text{H}_2\text{O}$ only.

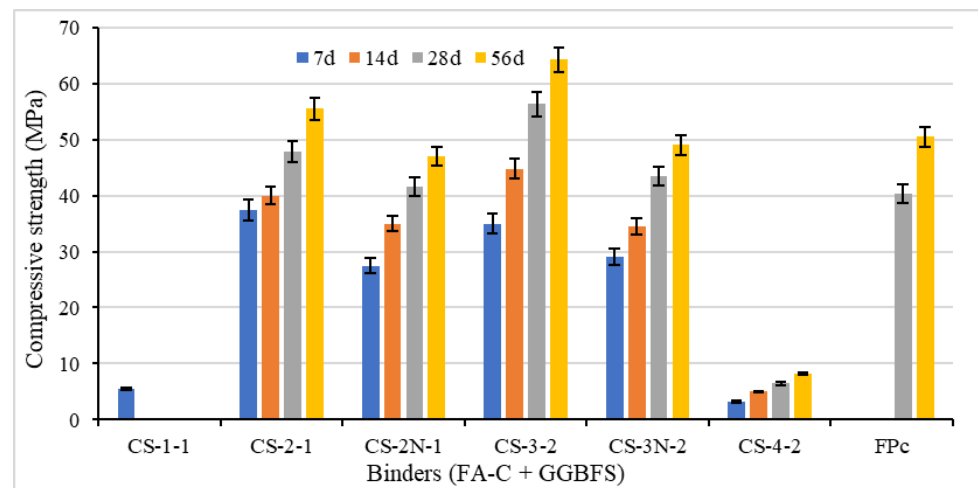


Figure 7. Influence of reagents (1 and 2) on binary binders (FA-C + GGBFS).

3.1.5. Influence of Powder-Based Reagents on Binary Combinations of FA-C, FA-F, and GGBFS Binders

The composition of $\text{Ca}(\text{OH})_2:\text{Na}_2\text{SiO}_3 \cdot 5\text{H}_2\text{O} = 2.5:1$ performed the best among the other component ratios for reagent-1, obtaining a compressive strength of 29.5 MPa at 56 days for the binder FS-2-1. This composition had the highest calcium content and the required alkalinity for the dissolution of the Si and Al, which resulted in 6 to 25% higher strengths than the reagent-1/1a-based mix compositions, as evident from Figure 8. The binary binder (FS-4-2) incorporating reagent-2 had setting times greater than 24 h and this correspondingly resulted in a low compressive strength of 4.3 MPa at 28 days. This could be due to the incompatibility between the reagent composition and the source material.

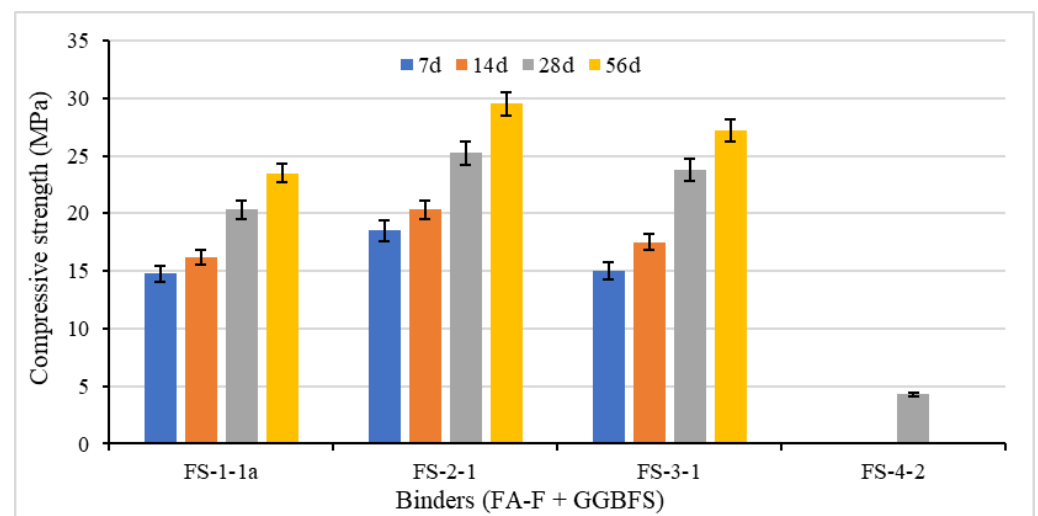


Figure 8. Influence of powder-based reagents on binary binders (FA-F + GGBFS).

The binary binders composed with FA-C and FA-F as precursors and different combinations/dosages of reagents, as illustrated in mix proportions presented in Table 5a,b, had long setting times (>24 h). These binder systems hence resulted in low compressive strengths ranging from 4 to 7.5 MPa at 28 days, respectively. These results can be attributed to the plausible leaching of Si and Al ions from the system, low reactivity of FA-F, and possible incompatibility of the reagent compositions with the binder systems.

3.1.6. Influence of Powder-Based Reagents on Ternary Combinations of FA-C, FA-F, and GGBFS Binders

The ternary binders with reagent-1 and 2 obtained compressive strengths ranging from 3.5 MPa to 52.2 MPa at 28 days. The reagent-1 component ratio of $\text{Ca}(\text{OH})_2:\text{Na}_2\text{SiO}_3 \cdot 5\text{H}_2\text{O} = 1:2.5$ was judged to be the optimal composition based on strength results (54.2 MPa at 56 days) of the binder system CFS-4-1. The high alkalinity of sodium metasilicate ($\text{pH} = 14$) resulted in the enhanced dissolution of Si and Al ions from FA-F, which otherwise shows low reactivity. Additionally, the presence of high-calcium precursors (GGBFS and FA-C) led to the formation of C-A-S-H binding phases which compacted the amorphous N-A-S-H, resulting in a dense microstructure and high compressive strengths. However, for reagent 2, a $\text{Ca}(\text{OH})_2/\text{Na}_2\text{SO}_4 = 2.5:1$ component ratio was determined to be superior, which also outperformed reagent-1, as depicted in Figure 9. The additional C-S-H gel formation owing to the presence of high levels of calcium in the system from the reagent-2 composition led to higher compressive strengths. The mix compositions CFS-4N-1 and CFS-5N-2 having a 10% higher GGBFS content than their counterparts CFS-4-1 and CFS-5-2 resulted in 8 to 25% less compressive strength at 28 days. A similar trend for compressive strength was observed for the binary binders (FA-C + GGBFS) having the same reagent compositions.

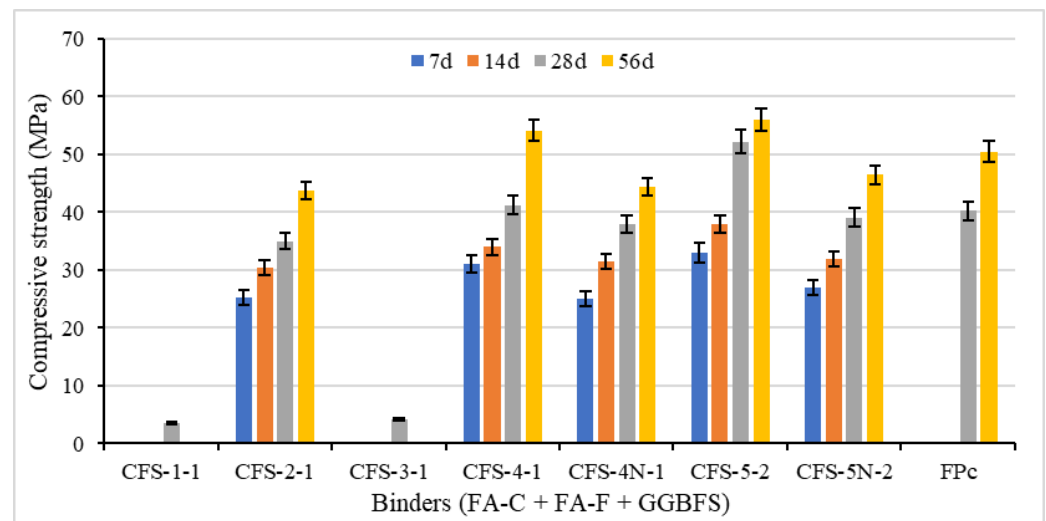


Figure 9. Influence of reagents (1 and 2) on ternary binders (FA-C + FA-F + GGBFS).

3.2. Identification Best Binder Compositions and Microstructural Analysis

Based on the 28-day compressive strength (Table 5a,b) and flow characteristics (mini-slump flow spread >155 mm), four binary binders (CS-2-1, CS-3-2, CS-2N-1, and CS-3N-2) with strength ranging between 41 MPa and 56 MPa, as well as four ternary binders (CFS-4-1, CFS-5-2, CFS-4N1, and CFS-5N-2) with strength ranging between 38 MPa and 52 MPa, are identified as the best mixes. These binders developed compressive strength higher than that (40 MPa) of control cement paste (FPC). In addition, four mono binders (C-10-1, S-2-1, S-3-2, and S-4-2) with 28-day compressive strength of 21MPa to 34 MPa can also be considered as lower strength alternatives. Considering the use powder-based components (promoting one-part technology) and application of ambient curing (avoiding traditional heat curing), these binders can be easily produced for practical applications.

The superior performance of two ternary binders (CFS-5-2 and CFS-4-1) incorporating reagent-2 and 1, respectively, in terms of better compressive strength characteristics are selected in this paper to assess microstructural characteristics using SEM, EDS, and XRD analyses to understand the effect of reagents and different precursors (FA-C, FA-F, and GGBFS) as well as the formation of different reaction products/mineral phases.

The ternary binders had comparatively more amorphous reaction products than the crystalline phases due to the high content of fly ash (25%FA-C+35%FA-F) in the binder composition, as depicted in SEM micrographs in Figure 10a,b, which was also verified from XRD analysis. The binder CFS-5-2 appears to be denser than CFS-4-1 due to a higher content of calcium in the system owing to the composition of reagent-2. Some partially/unhydrated round grains of fly ash and angular-shaped GGBFS can be seen embedded in the matrix.

Ternary binders (CFS) obtained lower strengths than binary binders (CS) owing to the larger particle size of FA-F. Many unhydrated/partially hydrated fly ash (FA-F) particles are seen in the CFS-4-1 micrograph due to their low reactivity owing to the presence of firm chains of Si-Al which need to be broken first to initiate the reaction (Figure 11a). The cylindrical Si-Al linkages can be seen in the SEM micrograph, with low-calcium N(C)-A-S-H gels being the main reaction products, as shown in Figure 11a, and the peaks in EDS also identified the presence of the composition elements.

The availability of a larger amount of Ca^{2+} ions from reagent-2 ($\text{Ca}(\text{OH})_2/\text{Na}_2\text{SO}_4 = 2.5:1$) and FA-F's intrinsic high silica content led to the formation of C-S-H in binder CFS-5-2. This additional binding phase further densified the pore structure, leading to the higher strength of CFS-5-2 (52.2 MPa at 28 days) compared to the CFS-4-1 binder (41.3 MPa). Similar reaction products/gels were seen in previous studies [52]. The main binding gel/phases observed were N(C)-A-S-H/C-A-S-H and N-A-S-H, as indicated in the micrograph and characterized by EDS, as shown in Figure 11b.

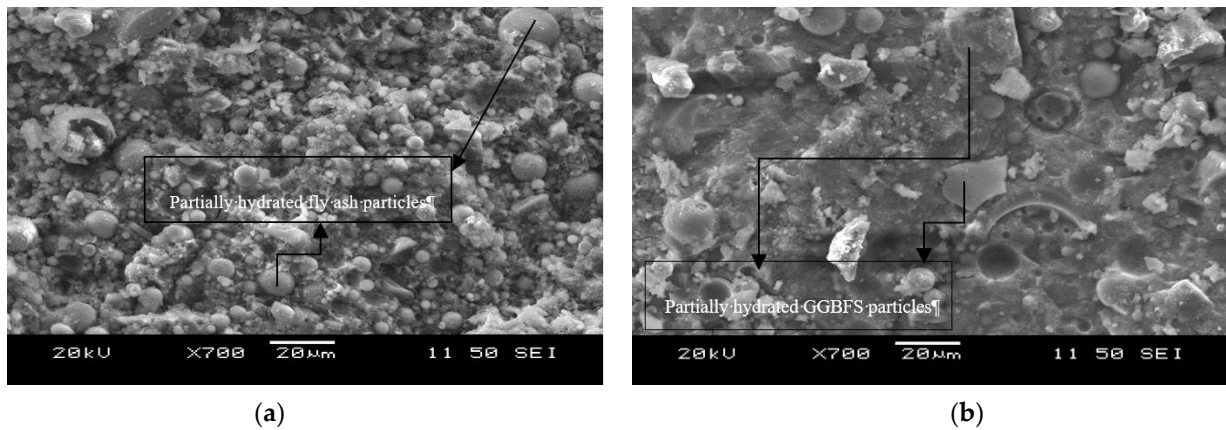


Figure 10. Morphology of binders using SEM (a) CFS-4-1; (b) CFS-5-2.

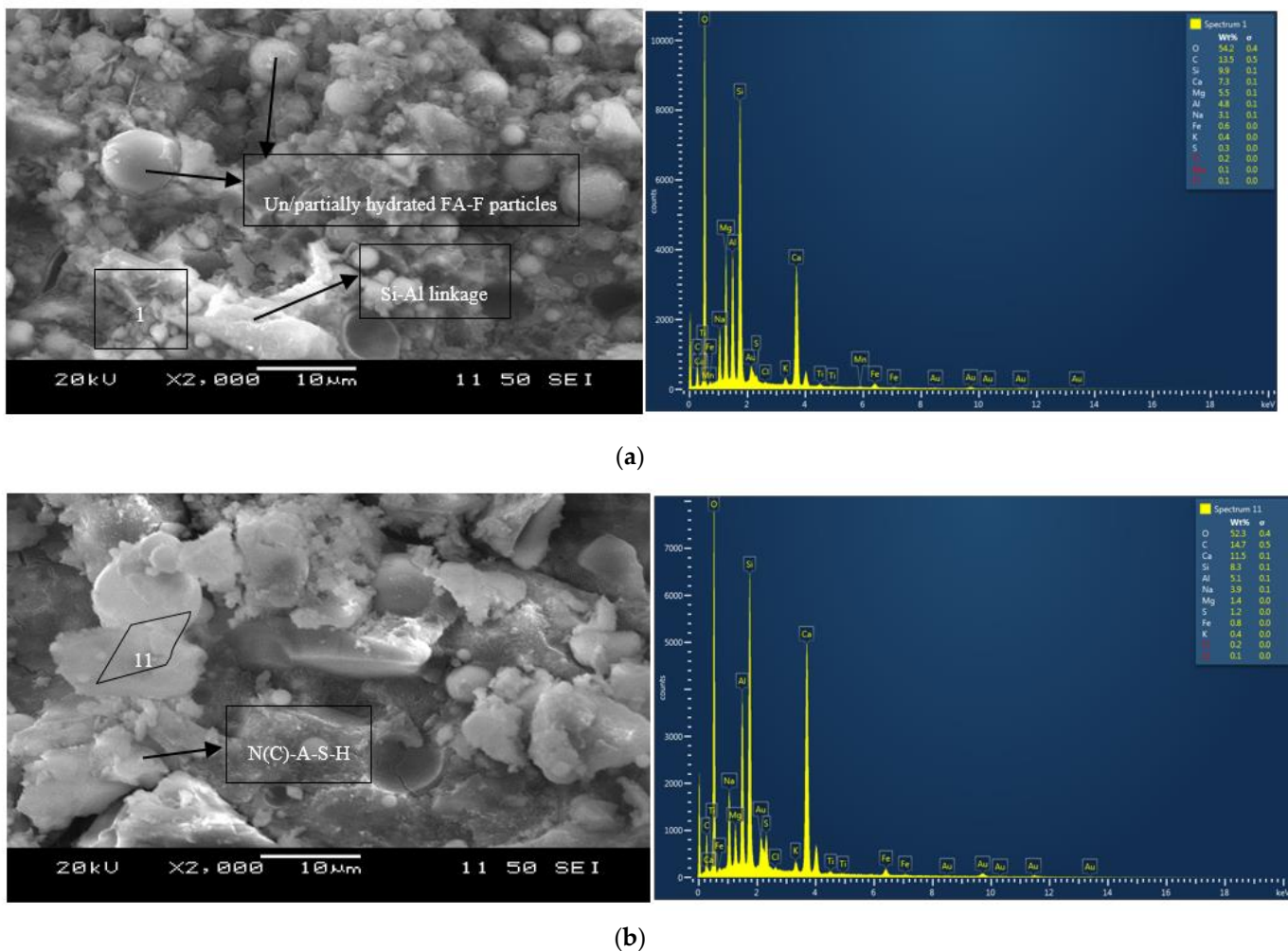


Figure 11. (a) SEM micrographs and EDS analysis of the ternary binder CFS-4-1. (b) SEM micrographs and EDS analysis of the ternary binder CFS-5-2.

The XRD diffractograms of the ternary binders (CFS-4-1 and CFS-5-2) incorporating reagent-1 and 2 are illustrated in Figure 12a,b and the mineral phases identified are presented in Table 6. These alkali-activated binders exhibited the formation of sodium or mixed Ca/Na compounds. The mineral phases consisted of quartz, calcite, and dolomite for CFS-5-2 with reagent-2, showing a larger number of peaks than the CFS-4-1 counterpart

with reagent-1. The binding phases composed of N-C-A-S-H/C-A-S-H were identified and determined as the main reaction products from the diffractograms and SEM/EDS analysis of binder CFS-5-2. Additionally, some phases of portlandite were seen in the CFS-5-2 ternary binder with reagent-2, indicating the presence of excessive calcium in the system. The highest peak representing quartz for CFS-4-1 and CFS-5-2 was observed at 29.7° 2θ. A combination of binding phases consisting of N-A-S-H/N-C-A-S-H as determined earlier in SEM/EDS analysis was also identified in the diffractogram of CFS-4-1. The dominant mineral phases consisted of lalondeite ((Na,Ca)₆(Ca,Na)₃Si₁₆O₃₈(F,OH)₂·3H₂O), grossular, quartz, and calcite from 26° 2θ to 38° 2θ, as presented in Figure 12a. Some traces of periclase (MgO) and gypsum were present in both the ternary binders. The presence of gypsum prevented the flash setting of mixes and MgO content in the mix compositions is known for counteracting shrinkage by its inherent expansive nature [45].

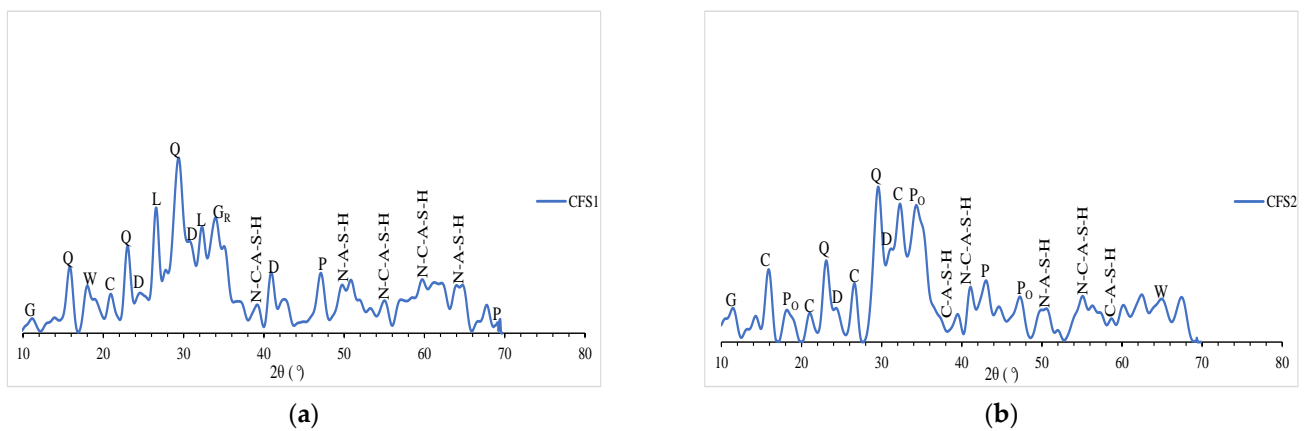


Figure 12. XRD patterns (a) CFS4-1; (b) CFS-5-2.

Table 6. Identified mineral phases in ternary binders.

Symbol	Name	Chemical Formula/Composition
C	Calcite	CaCO ₃
D	Dolomite	CaMg(CO ₃) ₂
G	Gypsum	CaSO ₄ ·2H ₂ O
G _R	Grossular	Ca ₃ Al ₂ (SiO ₄) ₃
L	Lalondeite	(Na,Ca) ₆ (Ca,Na) ₃ Si ₁₆ O ₃₈ (F,OH) ₂ ·3H ₂ O
P	Periclase	MgO
P _O	Portlandite	Ca(OH) ₂
Q	Quartz	SiO ₂
W	Wadalite	(Ca,Mg) ₆ (Al,Fe ³⁺) ₄ ((Si,Al)O ₄) ₃ O ₄ Cl ₃
C-A-S-H	Calcium-aluminate-silicate-hydrates	C, N, A, S and H denote CaO, Na ₂ O, Al ₂ O ₃ , SiO ₂ , and H ₂ O
C-S-H	Calcium-silicate-hydrate	
N-A-S-H	Sodium-alumino-silicate-hydrate	
N-C-A-S-H	Sodium-calcium-aluminate-silicate-hydrates	

4. Conclusions

The strength, workability, and microstructural characteristics of forty-four alkali-activated binders (AABs)/mixes incorporating mono, binary, and ternary combinations of supplementary cementitious materials (SCMs) (such as: fly ash class C (FA-C), fly ash class F (FA-F), and GGBFS) as precursors and incorporating six types of the multi-component

powdered/solution form of reagents/activators were studied. The combinations of sodium hydroxide (solution), calcium hydroxide (powder), sodium silicate (solution-grade D), sodium silicate (powder-grade G), sodium silicate (powder-grade GD), sodium metasilicate (powder), and sodium sulfate (powder) were used as single/multi-component reagents. The influences of different types/combinations/dosages of precursors and reagents on the compressive strength and workability properties of binders were assessed. The following conclusions are drawn from the study:

- (1) Binary (FA-C and GGBFS) and ternary (FA-C, FA-F, and GGBFS) binder compositions having a GGBFS content of 40% to 50% incorporating reagent-1 ($\text{Ca}(\text{OH})_2:\text{Na}_2\text{SiO}_3\cdot 5\text{H}_2\text{O} = 1:2.5$) and reagent-2 ($\text{Ca}(\text{OH})_2:\text{Na}_2\text{SO}_4 = 2.5:1$) were determined to be optimized compositions in terms of desired workability (slump flow spread >155 mm) and 28-day compressive strength (>38 MPa).
- (2) The utilization of multi-component reagents (combinations of calcium hydroxide with sodium silicates and sodium sulfate) was found to be favorable as compared to the incorporation of single component reagents (sodium silicates alone) in the development of binders. The use of single component reagents resulted in expansive product formation due to the presence of excessive sodium in the system.
- (3) Both binary (FA-C and GGBFS) and ternary binders having a GGBFS content of 40 to 45% obtained 8% to 34% higher compressive strengths than their counterparts having equal total fly ash and GGBFS content. Binary binder CS-3-2 composed of 55% FA-C and 45% GGBFS with reagent-2 (calcium hydroxide and sodium sulfate) obtained the highest compressive strength of 64.2 MPa at 56 days.
- (4) An increase in GGBFS content by 5% in binary binders and 10% in ternary binders resulted in an 8 to 25% reduction of compressive strength. There seems to be a threshold of GGBFS or calcium content in the system that governs the strength. GGBFS content of 45% in the mix compositions was determined to be optimal based on strength characteristics.
- (5) The incorporation of naphthalene-based superplasticizer (SP) in the development of GGBFS-based mono binders led to lower strengths at 7/14/28 days but produced similar strengths at 56 days compared to the binders using polycarboxylate-based SP.
- (6) The main binding phases/gels for ternary binders consisted of a combination of N-A-S-H or N(C)-A-S-H and C-A-S-H. The additional formation of C-S-H gel was observed for ternary binders with reagent-2 owing to the high calcium content of the reagent.
- (7) Four binary and four ternary one-part binders with 28-day compressive strength ranging between 38 MPa and 56 MPa and suitable workability are identified as the best and can be easily produced in the field using powder-based components and ambient curing conditions. On the other hand, heat curing is required in the two-part (conventional) binder to achieve similar strength in addition to the requirement for a larger amount of highly alkaline/corrosive solution-based reagents, and the handling of large quantities of solution-based reagents and precursors separately, which greatly hinders the ease of field production.
- (8) This study further reinforces the feasibility and commercial viability of sustainable alkali-activated binder development using the dry mixing technique based on fresh and hardened state characteristics.

Author Contributions: Conceptualization, K.M.A.H. and D.S.; Methodology, K.M.A.H. and D.S.; Software, D.S. and K.M.A.H.; Formal Analysis, D.S.; Investigation, D.S.; Resources, K.M.A.H.; Data Curation, D.S.; Writing-Original Draft Preparation, K.M.A.H. and D.S.; Writing-Review & Editing, K.M.A.H. and D.S.; Supervision, K.M.A.H.; Project Administration, K.M.A.H.; Funding Acquisition, K.M.A.H. All authors have read and agreed to the published version of the manuscript.

Funding: This research was funded by [Natural Science and Engineering Research Council (NSERC) Canada], grant number [RGPIN-2019-05613]

Acknowledgments: The authors gratefully acknowledge the financial support provided by the Natural Science and Engineering Research Council (NSERC), Canada.

Conflicts of Interest: The authors declare no conflict of interest.

References

1. Bong, S.H.; Nematollahi, B.; Nazari, A.; Xia, M.; Sanjayan, J. Efficiency of Different Superplasticizers and Retarders on Properties of “One-Part” Fly Ash-Slag Blended Geopolymers with Different Activators. *Materials* **2019**, *12*, 3410. [[CrossRef](#)]
2. Huseien, G.F.; Mirza, J.; Ismail, M.; Ghoshal, S.; Hussein, A.A. Geopolymer mortars as sustainable repair material: A comprehensive review. *Renew. Sustain. Energy Rev.* **2017**, *80*, 54–74. [[CrossRef](#)]
3. Zhang, P.; Zheng, Y.; Wang, K.; Zhang, J. A review on properties of fresh and hardened geopolymer mortar. *Compos. Part B Eng.* **2018**, *152*, 79–95. [[CrossRef](#)]
4. Elyamany, H.E.; Elmoaty, M.A.; Elshaboury, M.A. Setting time and 7-day strength of geopolymer mortar with various binders. *Constr. Build. Mater.* **2018**, *187*, 974–983. [[CrossRef](#)]
5. Zhou, W.; Yan, C.; Duan, P.; Liu, Y.; Zhang, Z.; Qiu, X.; Li, D. A comparative study of high- and low-Al₂O₃ fly ash based-geopolymers: The role of mix proportion factors and curing temperature. *Mater. Des.* **2016**, *95*, 63–74. [[CrossRef](#)]
6. Alnahhal, M.F.; Alengaram, U.J.; Jumaat, M.Z.; Alqedra, M.A.; Mo, K.H.; Sumesh, M. Evaluation of Industrial By-Products as Sustainable Pozzolanic Materials in Recycled Aggregate Concrete. *Sustainability* **2017**, *9*, 767. [[CrossRef](#)]
7. Baykara, H.; Cornejo, M.H.; Espinoza, A.; García, E.; Ulloa, N. Preparation, characterization, and evaluation of compressive strength of polypropylene fiber reinforced geopolymer mortars. *Heliyon* **2020**, *6*, e03755. [[CrossRef](#)] [[PubMed](#)]
8. El-Wafa, M.A.; Fukuzawa, K. Early-Age Strength of Alkali-Activated Municipal Slag-Fly Ash-Based Geopolymer Mortar. *J. Mater. Civ. Eng.* **2018**, *30*, 04018040. [[CrossRef](#)]
9. Wang, S.; Li, V.C. Engineered Cementitious Composites with High-Volume Fly Ash. *ACI Mater. J.* **2008**, *104*, 233–241.
10. Ng, C.; Alengaram, U.J.; Wong, L.S.; Mo, K.H.; Jumaat, M.Z.; Ramesh, S. A review on microstructural study and compressive strength of geopolymer mortar, paste and concrete. *Constr. Build. Mater.* **2018**, *186*, 550–576. [[CrossRef](#)]
11. Sood, D.; Hossain, K.M.A.; Manzur, T.; Hasan, M.J. Developing Geopolymer Pastes Using Dry Mixing Technique. In Proceedings of the 7th International Conference on Engineering Mechanics and Materials (CSCE 2019), Laval, QC, Canada, 12–15 June 2019; pp. 1–8.
12. Görhan, G.; Aslaner, R.; Şinik, O. The effect of curing on the properties of metakaolin and fly ash-based geopolymer paste. *Compos. Part B Eng.* **2016**, *97*, 329–335. [[CrossRef](#)]
13. Duxson, P.; Fernández-Jiménez, A.; Provis, J.L.; Lukey, G.C.; Palomo, A.; van Deventer, J.S.J. Geopolymer technology: The current state of the art. *J. Mater. Sci.* **2006**, *42*, 2917–2933. [[CrossRef](#)]
14. Provis, J.L. Geopolymers and other alkali activated materials: Why, how, and what? *Mater. Struct.* **2014**, *47*, 11–25. [[CrossRef](#)]
15. Shah, S.F.A.; Chen, B.; Oderji, S.Y.; Haque, M.A.; Ahmad, M.R. Comparative study on the effect of fiber type and content on the performance of one-part alkali-activated mortar. *Constr. Build. Mater.* **2020**, *243*, 118221. [[CrossRef](#)]
16. Shah, S.F.A.; Chen, B.; Oderji, S.Y.; Haque, M.A.; Ahmad, M.R. Improvement of early strength of fly ash-slag based one-part alkali activated mortar. *Constr. Build. Mater.* **2020**, *246*, 118533. [[CrossRef](#)]
17. Krivenko, P. Alkali Activated Cements versus Geopolymers. *Civ. Eng. Res. J.* **2017**, *1*, 4–6. [[CrossRef](#)]
18. Davidovits, J. Geopolymers. *J. Therm. Anal.* **1991**, *37*, 1633–1656. [[CrossRef](#)]
19. Wei, X.; Ming, F.; Li, D.; Chen, L.; Liu, Y. Influence of Water Content on Mechanical Strength and Microstructure of Alkali-Activated Fly Ash/GGBFS Mortars Cured at Cold and Polar Regions. *Materials* **2019**, *13*, 138. [[CrossRef](#)]
20. Samantasinghar, S.; Singh, S.P. Fresh and Hardened Properties of Fly Ash-Slag Blended Geopolymer Paste and Mortar. *Int. J. Concr. Struct. Mater.* **2019**, *13*, 47. [[CrossRef](#)]
21. Nematollahi, B.; Sanjayan, J.; Shaikh, F.U.A. Synthesis of heat and ambient cured one-part geopolymer mixes with different grades of sodium silicate. *Ceram. Int.* **2015**, *41*, 5696–5704. [[CrossRef](#)]
22. Abdollahnejad, Z.; Mastali, M.; Falah, M.; Shaad, M.K.; Luukkonen, T.; Illikainen, M. Durability of the Reinforced One-Part Alkali-Activated Slag Mortars with Different Fibers. *Waste Biomass Valorization* **2020**, *12*, 487–501. [[CrossRef](#)]
23. Alrefaei, Y.; Wang, Y.-S.; Dai, J.-G. The effectiveness of different superplasticizers in ambient cured one-part alkali activated pastes. *Cem. Concr. Compos.* **2019**, *97*, 166–174. [[CrossRef](#)]
24. Luukkonen, T.; Sreenivasan, H.; Abdollahnejad, Z.; Yliniemi, J.; Kantola, A.; Telkki, V.-V.; Kinnunen, P.; Illikainen, M. Influence of sodium silicate powder silica modulus for mechanical and chemical properties of dry-mix alkali-activated slag mortar. *Constr. Build. Mater.* **2020**, *233*, 117354. [[CrossRef](#)]
25. Nematollahi, B.; Sanjayan, J.; Qiu, J.; Yang, E.-H. High ductile behavior of a polyethylene fiber-reinforced one-part geopolymer composite: A micromechanics-based investigation. *Arch. Civ. Mech. Eng.* **2017**, *17*, 555–563. [[CrossRef](#)]
26. Alrefaei, Y.; Wang, Y.-S.; Dai, J.-G.; Xu, Q. Effect of superplasticizers on properties of one-part Ca(OH)₂/Na₂SO₄ activated geopolymer pastes. *Constr. Build. Mater.* **2020**, *241*, 01–14. [[CrossRef](#)]
27. Nematollahi, B.; Sanjayan, J.; Qiu, J.; Yang, E.-H. Micromechanics-based investigation of a sustainable ambient temperature cured one-part strain hardening geopolymer composite. *Constr. Build. Mater.* **2017**, *131*, 552–563. [[CrossRef](#)]
28. Alrefaei, Y.; Dai, J.-G. Tensile behavior and microstructure of hybrid fiber ambient cured one-part engineered geopolymer composites. *Constr. Build. Mater.* **2018**, *184*, 419–431. [[CrossRef](#)]

29. Hossain, M.A.; Hossain, K.M.A.; Manzur, T.; Hasan, M.J.; Sood, D. Fresh and Hardened Properties of Engineered Geo-Polymer Composite with MgO. In Proceedings of the 5th International Conference on Civil Structural and Transportation Engineering (ICCSTE '20), Virtual, Niagara, ON, Canada, 12–14 November 2020; pp. 1–8.
30. Samantasinghar, S.; Singh, S.P. Effect of synthesis parameters on compressive strength of fly ash-slag blended geopolymer. *Constr. Build. Mater.* **2018**, *170*, 225–234. [[CrossRef](#)]
31. Luukkonen, T.; Abdollahnejada, Z.; Yliniemia, J.; Kinnunen, P.; Illikainen, M. One-part alkali-activated materials: A review. *Cem. Concr. Res.* **2017**, *103*, 21–34. [[CrossRef](#)]
32. Provis, J.L. Alkali-activated materials. *Cem. Concr. Res.* **2018**, *114*, 40–48. [[CrossRef](#)]
33. Adesanya, E.; Ohenoja, K.; Luukkonen, T.; Kinnunen, P.; Illikainen, M. One-part geopolymer cement from slag and pretreated paper sludge. *J. Clean. Prod.* **2018**, *185*, 168–175. [[CrossRef](#)]
34. Khale, D.; Chaudhary, R. Mechanism of geopolymerization and factors influencing its development: A review. *J. Mater. Sci.* **2007**, *42*, 729–746. [[CrossRef](#)]
35. Pan, Z.; Tao, Z.; Cao, Y.; Wuhner, R.; Murphy, T. Compressive strength and microstructure of alkali-activated fly ash/slag binders at high temperature. *Cem. Concr. Compos.* **2018**, *86*, 9–18. [[CrossRef](#)]
36. Kovalchuk, O.; Drochytka, R.; Krivenko, P. Mix Design of Hybrid High-Volume Fly Ash Alkali Activated Cement. *Adv. Mater. Res.* **2015**, *1100*, 36–43. [[CrossRef](#)]
37. Çelikten, S.; Sarıdemir, M.; Deneme, I.Ö. Mechanical and microstructural properties of alkali-activated slag and slag + fly ash mortars exposed to high temperature. *Constr. Build. Mater.* **2019**, *217*, 50–61. [[CrossRef](#)]
38. Yang, K.H.; Song, K.J.; Ashour, F.A.; Lee, T.E. Properties of cement less mortars activated by sodium silicate. *Constr. Build. Mater.* **2008**, *22*, 1981–1989. [[CrossRef](#)]
39. Provis, J.L.; Bernal, S.A. Geopolymers and Related Alkali-Activated Materials. *Annu. Rev. Mater. Res.* **2014**, *44*, 299–327. [[CrossRef](#)]
40. Provis, J.L.; Palomo, A.; Shi, C. Advances in understanding alkali-activated materials. *Cem. Concr. Res.* **2015**, *78*, 110–125. [[CrossRef](#)]
41. Chi, M. Effects of dosage of alkali-activated solution and curing conditions on the properties and durability of alkali-activated slag concrete. *Constr. Build. Mater.* **2012**, *35*, 240–245. [[CrossRef](#)]
42. Dong, M.; Elchalakani, M.; Karrech, A. Development of high strength one-part geopolymer mortar using sodium metasilicate. *Constr. Build. Mater.* **2020**, *236*, 117611. [[CrossRef](#)]
43. Deb, P.S.; Nath, P.; Sarker, P.K. The effects of ground granulated blast-furnace slag blending with fly ash and activator content on the workability and strength properties of geopolymer concrete cured at ambient temperature. *Mater. Des.* **2014**, *62*, 32–39. [[CrossRef](#)]
44. Ma, C.; Zhao, B.; Guo, S.; Long, G.; Xie, Y. Properties and characterization of green one-part geopolymer activated by composite activators. *J. Clean. Prod.* **2019**, *220*, 188–199. [[CrossRef](#)]
45. Sherir, M.A.; Hossain, K.M.A.; Lachemi, M. Self-healing and expansion characteristics of cementitious composites with high volume fly ash and MgO-type expansive agent. *Constr. Build. Mater.* **2016**, *127*, 80–92. [[CrossRef](#)]
46. Sherir, M.A.; Hossain, K.M.A.; Lachemi, M. Permeation and Transport Properties of Self-Healed Cementitious Composite Produced with MgO Expansive Agent. *J. Mater. Civil Eng.* **2018**, *30*, 1–19. [[CrossRef](#)]
47. ASTM C109/C109M. *Standard Test Method for Compressive Strength of Hydraulic Cement Mortars (Using 2-in. or [50-mm] Cube Specimens)*; ASTM International: West Conshohocken, PA, USA, 2016.
48. ASTM C1437. *Standard Test Method for Flow of Hydraulic Cement Mortar*; ASTM International: West Conshohocken, PA, USA, 2015.
49. Longhi, M.A.; Zhang, Z.; Rodriguez, E.D.; Kirchheim, A.P.; Wang, H. Efflorescence of Alkali-Activated Cements (Geo-Polymers) and the Impacts on Material Structures: A Critical Analysis. *Front. Mater.* **2019**, *6*, 89. [[CrossRef](#)]
50. Nematollahi, B.; Sanjayan, J.; Shaikh, F.U.A. Tensile Strain Hardening Behavior of PVA Fiber-Reinforced Engineered Geopolymer Composite. *J. Mater. Civil Eng.* **2015**, *27*, 1–12. [[CrossRef](#)]
51. Chi, M.; Huang, R. Binding mechanism and properties of alkali-activated fly ash/slag mortars. *Constr. Build. Mater.* **2012**, *40*, 291–298. [[CrossRef](#)]
52. Sasui, S.; Kim, G.; Nam, J.; Koyama, T.; Chansomsak, S. Strength and Microstructure of Class-C Fly Ash and GGBS Blend Geopolymer Activated in NaOH & NaOH+ Na₂SiO₃. *Materials* **2020**, *13*, 59. [[CrossRef](#)]